Tech Science Press

Design and Implementation of Wheel Chair Control System Using Particle Swarm Algorithm

G. Mousa[1], Amr Almaddah[2] and Ayman A. Aly[3,*]

[1]Mechanical Engineering Department, College of Engineering, King Abdulaziz University, Jeddah, 21589, Saudi Arabia
[2]Electrical and Computer Engineering, College of Engineering, King Abdulaziz University, Jeddah, 21589, Saudi Arabia
[3]Mechanical Engineering Department, College of Engineering, Taif University, Taif, 21944, Saudi Arabia
*Corresponding Author: Ayman A. Aly. Email: draymanelnaggar@gmail.com

Abstract: About 10–20% of every country's population is disable. There are at least 650 million people with a kind of disability worldwide. Assistance and support are perquisites for many handicap people for participating in society. Electric powered wheelchairs provide efficient mobility to motor impaired persons. In this paper a smart controller of a wheel chair mobile robot using Particle Swarm Optimization Proportional controller (*PSO-P*) was proposed where (*PSO*) algorithm was utilized to tune the proportional controller's gains for each axis. Aiming to improve wheelchair tracking trajectory, a kinematic model of a robot with linear and angular velocities parameters was developed. The controller performance was examined using the system parameters with respect to trajectory references. A simulation of the proposed controller showed good correlation of the trajectory track under different loading conditions.

Nomenclature

c_{ij}	center parameters of the MFs
$E(i)$	cost functions for i^{th} particle
$e_1(i)$	1st joint error
$e_2(i)$	2nd joint error
F	generalized force.
$gbest$	global best position of particle
I_c	chair moment of inertia.
i^{th}	particle sample
I_m	wheel and motor moment of inertia around the wheel diameter.
I_w	wheel and motor moment of inertia around the wheel axis.
j	iteration number.

K_{p1}	control gain of axis1
K_{p2}	control gain of axis2
l	vector position of wheel chair frame and reference frame
L	Lagrange function
MAE	magnitude of the error
m_c	mass the chair only.
m_w	wheel and motor mass.
N	sample number
$pbest$	best position of particle
p_i	i^{th} particle position
q	generalized coordinates
T_c	kinematic energy of wheel chair
t_f	final time
T_{wL}	left axis kinematic.
T_{wR}	right axis kinematic.
V	potential energy of wheel chair
v_i	i^{th} particle velocity
v_L	left wheel velocity
v_R	right wheel velocity
$(X_I ; Y_I)$	motion reference frame
$(X_R; Y_R)$	wheel chair frame
θ	angular position of wheel chair frame and reference frame
$\dot{\varphi}_1$	speed of axis1
$\dot{\varphi}_2$	speed of axis2
ω	system angular velocity
σ_{ij}	deviation parameters of the MFs
$\dot{\varepsilon}_t$	kinematic model for the wheel chair

1 Introduction

In Saudi Arabia, about 800,000 of the population suffer from moving disability. 100,000 of those are with extreme disability conditions [1]. According to the World Bank Organization 1 billon of the world population has some sort of disability. About 15% of those suffer significant disability conditions. This shows the importance of equipment and devices that are designed to deal with disabled people. In lack of such devices, social, economic conditions and important life matters interrupt severally. Electric wheelchair can ease such interruption where patents and alders can use it independently in their mobility. Electric carts are also becoming popular in tasks that are dangerous or troublesome for humans. It can replace workers in wide range of environments starting from factories to military and space exploration missions. Controllers differ with the verities of applications of carts. For instance, specifications of a warehouse trajectory are different than the trajectory of a warzone where maneuvering is needed to be precise. Such differences can be accumulated in the design of the controller.

The effort of improving electric wheelchairs and carts control is continually developed by researchers. In Emam et al. [2–4] developed controllable dynamic models. In [5] a model that considers the incline surface was proposed. Kirby et al. [6,7] considered stability in their model and its effect in performance and handling. Brown et al. [8] produced a PID control that is currently an industry standard for joy-stick controls of electric powered mobile chairs where it provides better management, handling and control overall.

Although the classical controllers have gained widespread usage across technological industries, it must also be pointed out that the unnecessary mathematical rigorosity, preciseness and accuracy involved with the design of controllers have been a major drawback. Designing and tuning a conventional controller appears to be conceptually intuitive, but can be hard in practice, if multiple objectives are to be achieved [9]. However, it is quite difficult to determine its optimum gains where systems are usually non-linear. Non-conventional control methods have been used to select the optimum desired motion of a controlled system where the minimal settling time with no overshoot is needed [10].

In this paper, *proportional (P)* controller tuning is attempted using the *PSO* algorithm which was introduced by Kennedy et al. [11]. The main advantage of this algorithm; it does not require detailed mathematical description of the process and finds the best possible control parameters based on the fitness function provided to guide the algorithm. A detailed study is presented with a *PSO-P* algorithm using various inertia weights.

The purpose of the research is to achieve a good control trajectory performance in terms of the system error and robustness for the system uncertainties. In this article, the dynamic model of the wheelchair will be introduced in Section 2. Then A *PSO-P* control strategy is suggested in Section 3. After that the *PSO*-adjusting policy for the *P*-control is illustrated in Section 4. Finally the results and conclusion are described in last Sections of 5 and 6.

2 Wheel Chair Model

The wheel chair as shown in Fig. 1 has 2 axes wheels. The center between the 2 axes is point P, the distance from point P to each wheel is l, θ is the angular position between wheel chair frame $(X_R; Y_R)$ and reference frame $(X_I; Y_I)$. Also r; l, θ, and $'\dot{\varphi}_1$ and $'\dot{\varphi}_2$ are the speeds of the 2 axes.
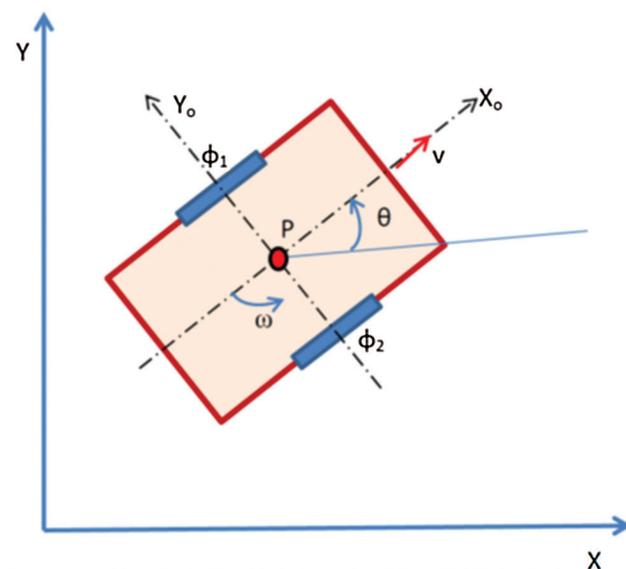

Figure 1: Wheel chair model

To perform the controlled movement of the wheel chair, the dynamic model of the system should be known. The Lagrange dynamic approach is showed systematically derives the equations of system motion [12,13].

Lagrange is a popular formulating approach for the governing equations of wheel chair motion. The general Lagrange equation is introduced by (1):

$$d/dt\left(\partial L/\partial \dot{q}_i\right) + \partial L/\partial \dot{q}_i = \tau \tag{1}$$

where: $L = T_c - V$; T is the kinematic energy of wheel chair; V is the potential energy; F is the generalized force.

The generalized coordinates q is chosen as:

$$q = \begin{bmatrix} x_p & y_p & \theta & \varnothing_R & \varnothing_L \end{bmatrix}^\wedge T \tag{2}$$

The kinetic energy is formulated as:

$$T_c = (1/2)\left[m_c(v_c)^\wedge 2 + I_c(\dot{\theta})^\wedge 2\right] \tag{3}$$

$$T_{wR} = (1/2)\left[m_w(v_w)^2 + I_m\left(\dot{\theta}\right)^2 + I_w(\dot{\varnothing}_R)^\wedge 2\right] \tag{4}$$

$$T_{wL} = (1/2)\left[m_w(v_w)^\wedge 2 + I_m(\dot{\theta})^\wedge 2 + I_w(\dot{\varnothing}_L)^\wedge 2\right] \tag{5}$$

where

T_{wR}: The right axis kinematic.

T_{wL}: The left axis kinematic.

m_c: The mass of the chair only.

m_w: The wheel and motor mass.

I_c: The chair moment of inertia.

I_w: The wheel and motor moment of inertia around the wheel axis.

I_m: The wheel and motor moment of inertia around the wheel diameter.

The axes velocities are formulated as:

$$v_i^{\wedge}2 = \dot{x}_i^{\wedge}2 + \dot{y}_i^{\wedge}2 \tag{6}$$

The coordinates of wheels can be presented as:

$$x_{wR} = x_p + l\,sin\,\theta, \quad y_{wR} = y_P + l\,cos\,\theta, \tag{7}$$

$$x_{wL} = x_p - l\,sin\,\theta, \quad y_{wL} = y_P + l\,cos\,\theta, \tag{8}$$

From (3) to (8) overall kinematic energy of the system can be formulated as:

$$T = (1/2)(m_c + 2m_w)\left(\dot{x}_p^{\wedge}2 + \dot{y}_p^{\wedge}2\right) - m_c d\dot{\theta}(\dot{y}_a\,cos\,\theta - \dot{x}_a\,sin\,\theta) + 1/2[I\dot{\theta}^{\wedge}2 + I_w(\dot{\varphi}_R^{\wedge}2 + \dot{\varphi}_L^{\wedge}2)] \tag{9}$$

2.1 Kinematic Model

The wheeled chair moves on a horizontal level which is described by the position of the mobile chair and the angular difference [14].

The rotation matrix of the chair position is formulated as:

$$R(\theta) = \begin{pmatrix} \cos\theta & \sin\theta & 0 \\ -\sin\theta & \cos\theta & 0 \\ 0 & 0 & 1 \end{pmatrix} \tag{10}$$

This rotation matrix describes the motion reference frame $\{X_I; Y_I\}$ to local frame $\{X_R; Y_R\}$. The velocity of each driving wheel in the system can be the average of the left and right wheel velocities.

$$v = (v_R + v_L/2) = (r\dot{\varphi}_1 + r\dot{\varphi}_2)/2 \tag{11}$$

Also the system angular velocities:

$$\omega = (v_R - v_L)/2l = (r\dot{\varphi}_1 - r\dot{\varphi}_2)/2l \tag{12}$$

Gathering the previous formulas, a kinematic model for the wheel chair can formulated as:

$$\dot{\varepsilon}_t = R(\theta)^{-1\dot{\varepsilon}_R} = R(\theta)^\wedge(-1)\begin{bmatrix} r\dot{\varphi}_1 + r\dot{\varphi}_2/2 \\ r\dot{\varphi}_1 - r\dot{\varphi}_2/2 \end{bmatrix} \tag{13}$$

It is supposed $\dot{y}_R$ is always zero because there is no sideways motion.

3 Control Design

The traditional method for finding the optimum tuning of control system parameters is to optimize the system model for each parameter and decide the characteristics of the system which give local optimum solution. This method may lead to solutions far away from the optimum as the method strongly depends on the peculiarities of the system and the intuition of the modeler. Thus, different approaches to optimize the control system to find global optimum solution are needed.

Aly [15] implemented the Genetic Algorithm (*GA*) to optimize PID parameters. The controller was verified on the state space model of servovalve attached to a rotary hydraulic actuator which is highly nonlinear dynamic system. The appropriate specifications of the GA for the rotary position control of an actuator system were presented. It is found that the optimal values of the feedback gains can be obtained within 10 generations, which corresponds to about 200 experiments. Also this strategy was verified again to optimize the control parameters of fire tube boiler [16]. The effect and violability of the Genetic-PID (*GPID*) control system and comparison with conventional control methods such as PID were investigated by nonlinear dynamic model simulation. In another challenge, the tuning of PD controller parameters for handling rigid spatial manipulators using *GA* was presented in [17]. A new fitness function was implemented to optimize the feedback gains and its efficiency was verified for control such nonlinear coupled system.

Compared with *GAs*, the information sharing mechanism in *PSO* is significantly different. In *GAs*, chromosomes share information with each other. So the whole population moves like a one group towards an optimal area [16]. In *PSO*, only *gbest* gives out the information to others. It is a one -way information sharing mechanism. The evolution only looks for the best solution. Compared with *GA*, all the particles tend to converge to the best solution quickly even in the local version in most cases.

In this study, the control design has two steps. The first step is finding the P controller gains using PSO algorithm which is search algorithms. The second step is applying the designed *P* to the wheel chair system with different trajectories references to grantee the stability and vanish the error of the system. Fig. 2 illustrates the system structure. The proposed control calculates the desired velocity (v_d), angular velocity (ω_d) according to the required position of the trajectory. The desired velocities (v_d), and (ω_d) will be the input to wheel chair dynamics which will use those values to produce the final velocities (v) and (ω) signals. In the next section, the *P* gains will be determined using *PSO* algorithm. In this section, *PSO* strategy is as shown in Fig. 3 to design P control parameters for a two axis robot to follow the reference trajectory.
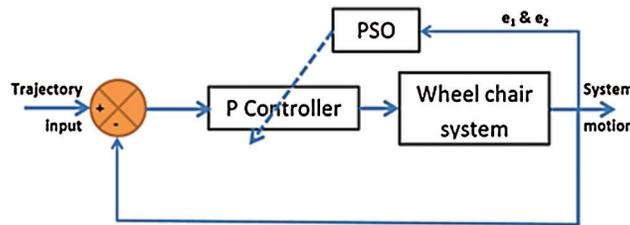
Figure 2: The overall system

3.1 Particle Swarm Optimization

Developmental computational strategy is dependent on the development and insight of multitudes searching for the most fertile feeding location. A "swarm" is an obviously disrupted assortment (populace) of moving individual that will in general bunch together while every individual is by all accounts moving an irregular way. It utilizes various specialists (particles) that establish a swarm moving around in the quest space searching for the best arrangement [12]. Each particle is handled as a point in an n-dimensional space which modifies its "flying" as per its own flying experience just as the flying experience of different particles. Every molecule monitors its directions in the issue space which are related with the best arrangement (fitness) that has accomplished up until now. This value is *pbest*. Another best value that is followed by the *PSO* is the best value got so far by any particle in the neighbors of the particle. This value is *gbest* [13,14].

The *PSO* idea comprises of variation the speed (or its rate) of each particle toward its *pbest* and the *gbest* position at each time step. Every particle attempts to adjust its present position and speed as per the distance between its present position and *pbest*, and the distance between its present position and *gbest* as demonstrated the following. At every progression *n*, by utilizing the individual best position, *pbest*, and global best position, *gbest*, a new speed for the *i*th particle is refreshed.

The speed is restricted to the scope of $[-v_{max}, +v_{max}]$. On the off chance that the speed disregards these cutoff points, it is compelled to its appropriate values. Changing speed by along these lines empowers the *i*th particle to look for its topical best position, *pbest*, and global best position, *gbest*. In light of the refreshed speed, every particle updates its situation as:

$$p_i(n) = p_i(n-1) + v_i(n) \tag{14}$$

In Fig. 4a, the particle position trip during the iteration process for K_{p1} of the first control axis while in Fig. 4b for the particle of second control axis K_{p2}.

Fig. 5a shows the particle velocity trip during the iteration process for K_{p1} of the first control axis and Fig. 5b shows for the particle of second control axis K_{p2}. It ought to be noticed that the estimations of an element in the particle may surpass its sensible range. This calculation is continued until most extreme cycle is attainable as illustrated in Fig. 6.

PSO look through the entirety of the forerunner and resulting parameters in 50 dimensional spaces. The order of a particle is illustrated as:

$$p_i = [\sigma_{11}c_{11} \ldots \ldots \sigma_{15}c_{15}\sigma_{21}c_{21} \ldots \ldots \sigma_{nn}c_{nn}] \tag{15}$$

where the σ_{ij} and c_{ij} represent the center and deviation parameters of the MFs. The underlying estimations of particles are haphazardly created in the first generation.
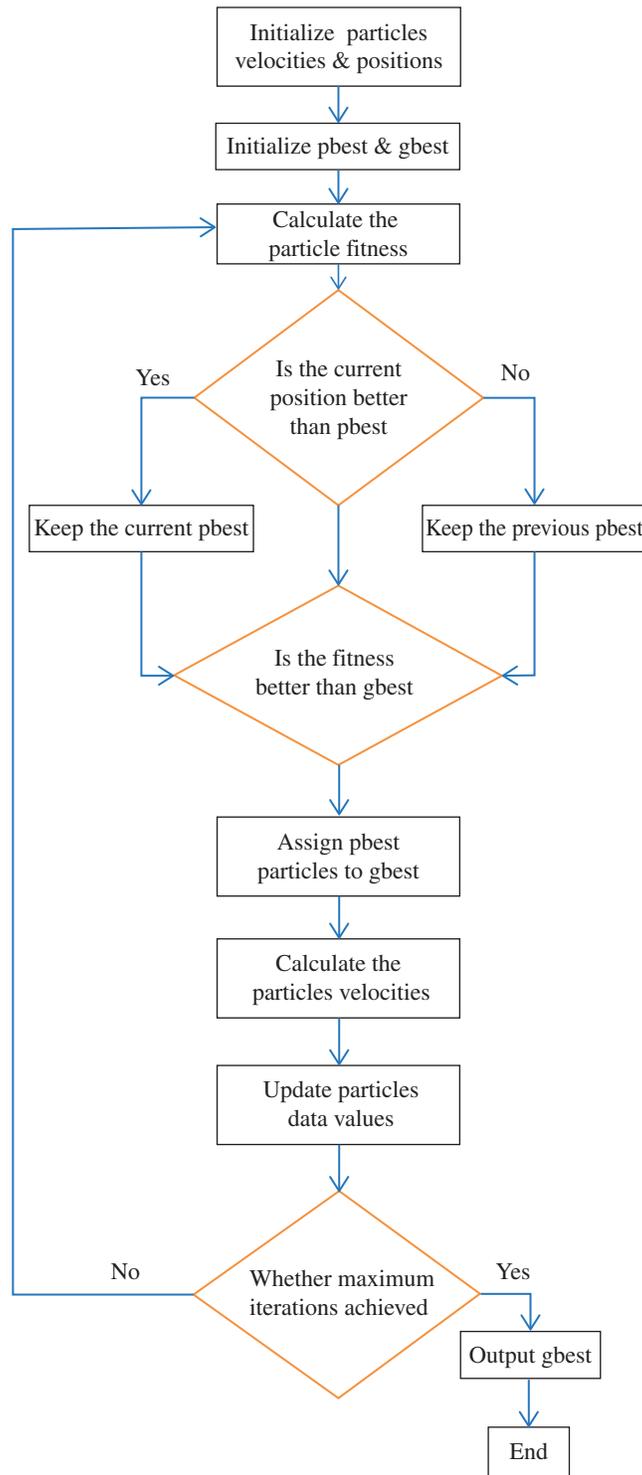
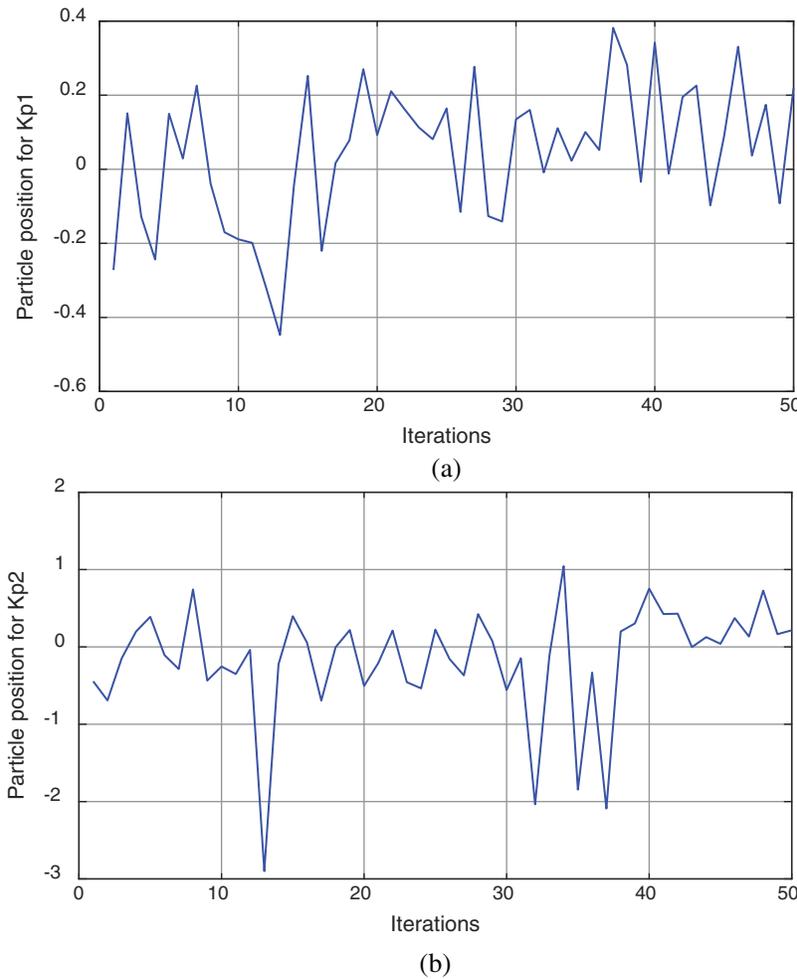**Figure 3:** Flow diagram illustrating the PSO algorithm

Figure 4: The particle position trip during the iteration process: (a) for K_{p1}; (b) for K_{p2}
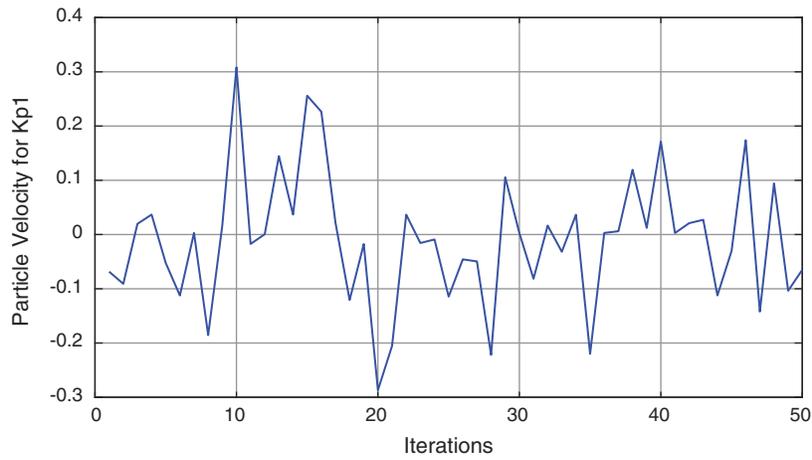
The important step in implementing *PSO* is to find the best fitness function which is utilized to estimate cost of every particle. While adjusting steps is running with *PSO*, Magnitude of the Error (*MAE*) is utilized as a cost function, which is illustrated in Fig. 6. The cost functions for *i*th particle are calculated as:

$$MAE = E(j) = \frac{1}{N} \sum_{i=1}^{n} |e_1(i)| + |e_2(i)| \tag{16}$$

where $e_1(i)$ is the *1*st joint error, $e_2(i)$ is the *2*nd joint error of *i*th sample, N is the sample number, j is the iteration number.

The population size is chosen to be *10* particles for each axis for minimizing calculations effort, the cost function is computed for each particle and *pbest* and *gbest* are calculated for each final time (t_f). A particle speed is computed for every particle and a particle position as follows:

$$\begin{aligned} v_{i,j}^{k+1} &= v_{i,j}^{k} + c_1 * r_1 * \left(pbest_{i,j}^{k} - x_{i,j}^{k} \right) + c_2 * r_2 \ * \left(gbest_{i,j}^{k} - x_{i,j}^{k} \right) x_{i,j}{}^{\wedge}(k+1) \\ &= x_{i,j}{}^{\wedge}(k) + v_{i,j}{}^{\wedge}(k+1) \end{aligned} \tag{17}$$

Figure 5: The particle velocity trip during the iteration process: (a) for K_{p1}; (b) for K_{p2}
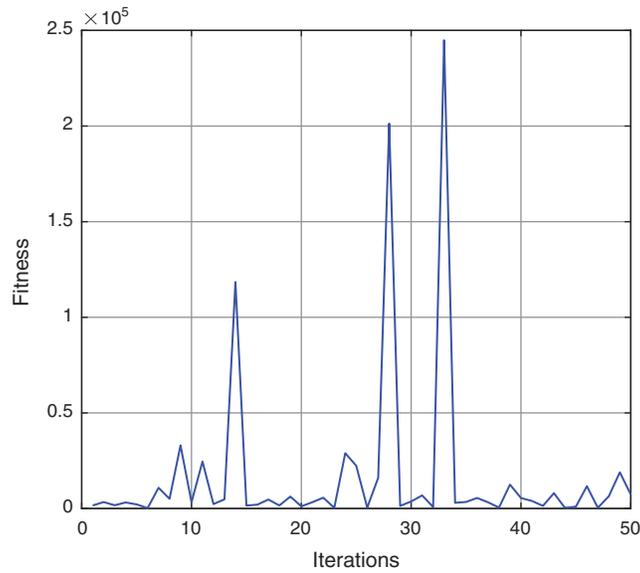

Figure 6: Fitness magnitude of the error (*MAE*)

4 Results

To illustrate the system behavior under the proposed controller several standard test commands such as fixed point, line, and circle inputs are applied to the system. The responses of *PSO-P* controller are illustrated below. The performance of the control system through a set of simulations was examined. The values of k_{p1}, and k_{p2}, are found by *PSO* strategy.

For testing the controller performance, different three dynamic loads are used from references of [18–21] with different loads of 10 kg, 55 kg and 125 kg respectively. The control was designed based on the dynamics of a Pioneer 2-DX wheel chair [13] weighing of 10 kg. Then the system performance was examined two times by change the dynamic load of the system to be 55 kg and 125 kg, which changes its dynamics behavior from that of the Pioneer 2-DX significantly.

In the simulation, the mobile chair reaches fixed point from its original position, while another test is starting from its original position and moving to be closed with reference line and final test that the robot should follow a circular trajectory of reference.

4.1 Fixed Point Input

Fig. 7 illustrates the response of the wheel chair system based on *PSO-P* for a reference fixed point input with test conditions of max linear velocity acceleration in both axis are 0.9 m/s and 0.5 m/s^2 while max rotation velocity of 1.9 rad/s. The obtained results for fixed point of (1.0 m, 1.0 m) has settling time about of (54 s for payload of 10 and 55 kg) while for the dynamic load of 125 kg the settling time increased. The steady state error changed from about zero second to be 0.066 m when the dynamics parameters of payload of 125 kg was implemented as presented in Fig. 8. The Cartesian components of polar trajectory were illustrated at Figs. 9a, 9b with steady state error in X axis is approximately 0.05 m and in y axis 0.043 m while the velocities were illustrated in Figs. 10a, 10b for both of linear and rotary under the maximum designed values.
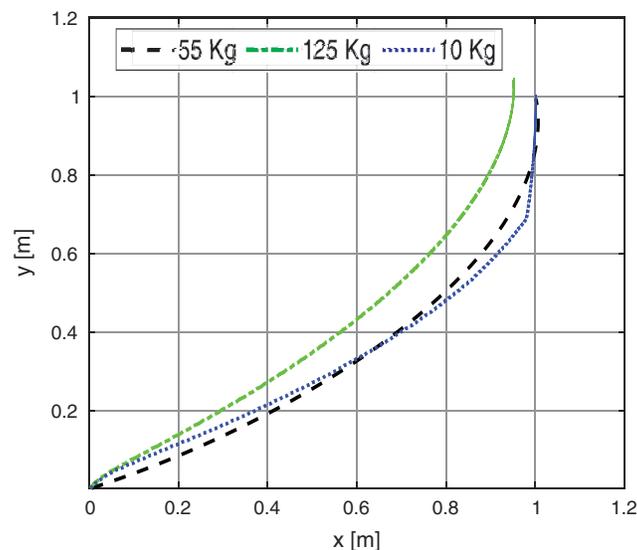

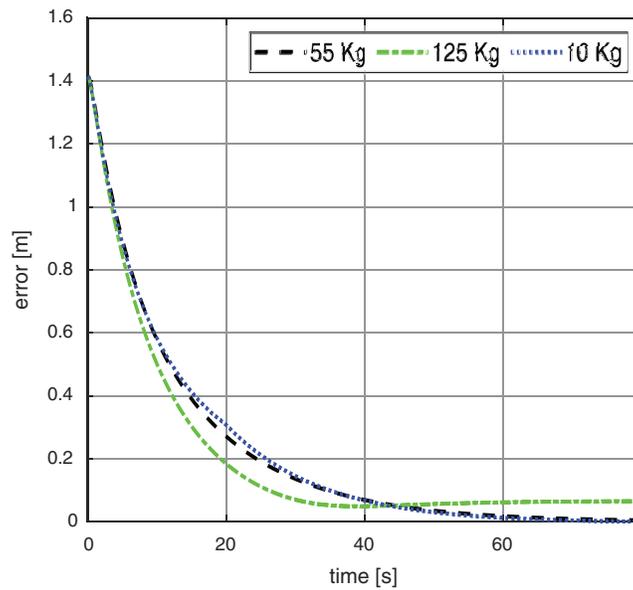**Figure 7:** The system response based on fixed point reference with different payloads

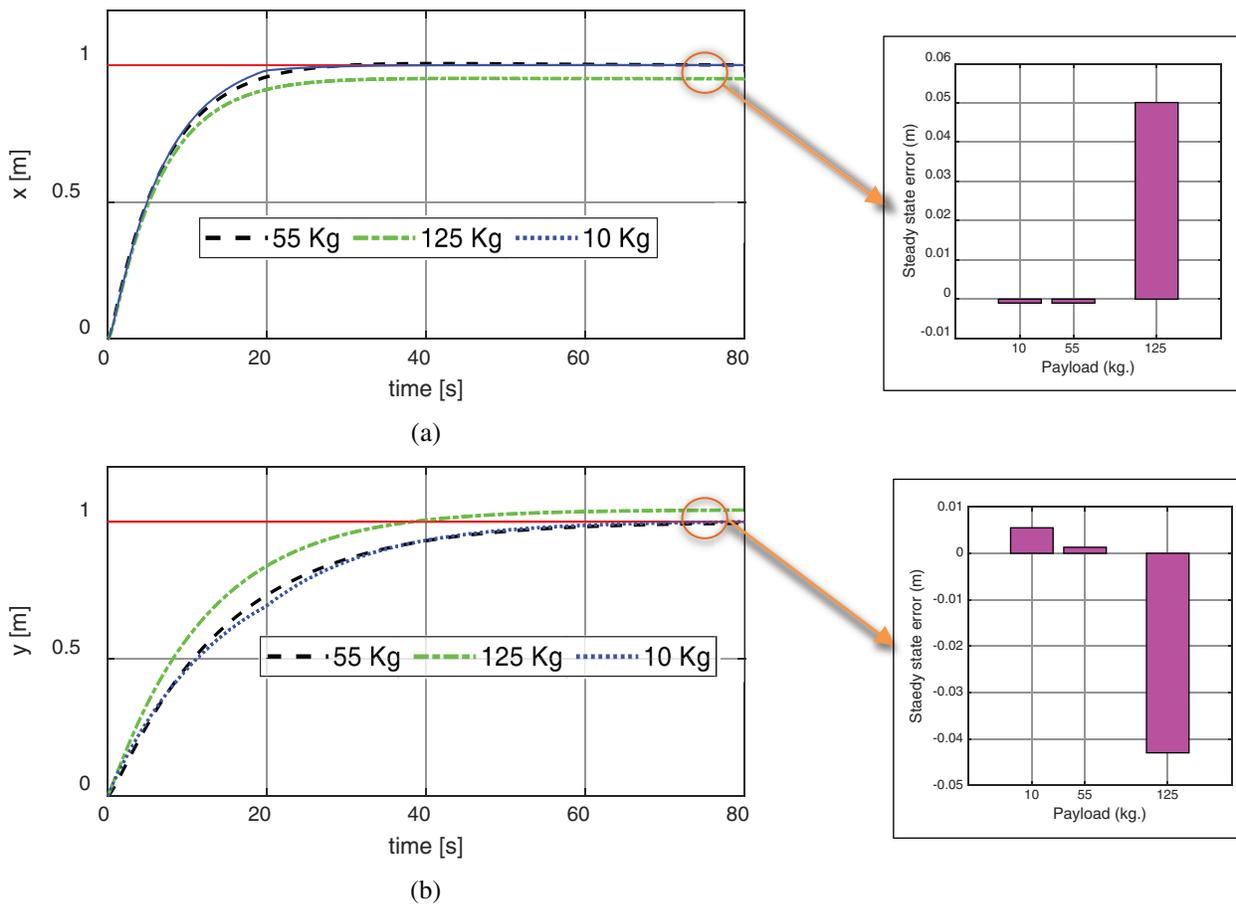**Figure 8:** The system response error based on fixed point reference with different payloads

(a)

(b)

Figure 9: The system Cartesian response based on fixed point reference with different payloads: (a) X-axis; (b) Y axis
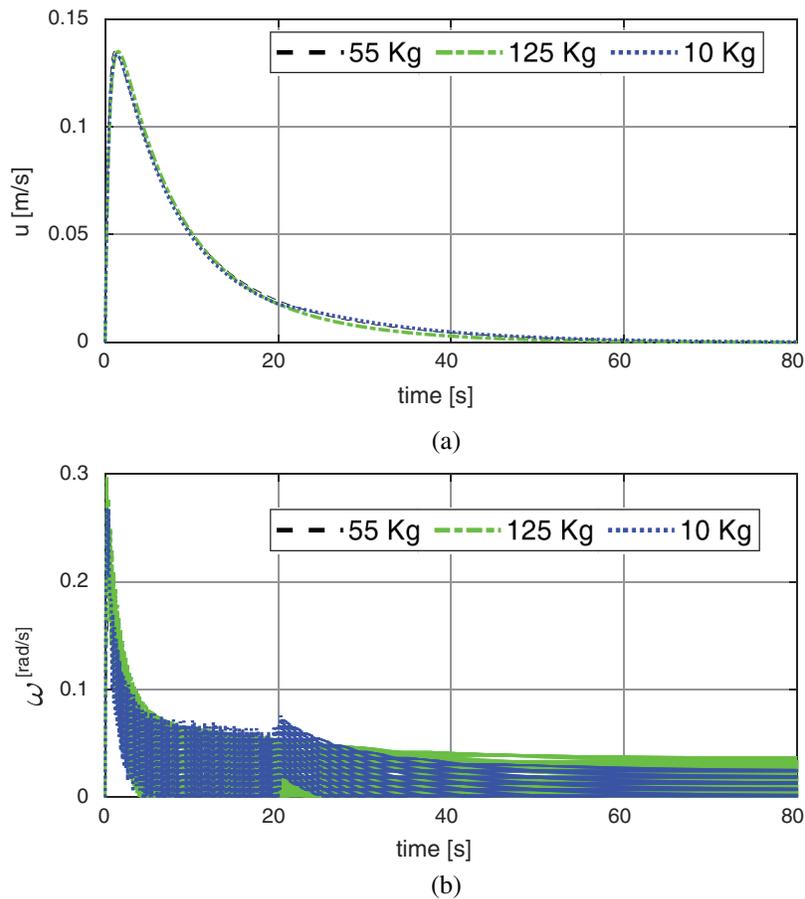
(a)

(b)

Figure 10: The system velocities based on fixed point reference with different payloads: (a) Linear velocity; (b) Rotary velocity

4.2 Line Input

Figs. 11, 12 shows another test with path reference as line input (x = 1) of the wheel chair system based on *PSO-P* controller. The path tracking is closer to the input command with about zero for 10 kg, 0.01 m for 55 kg and 0.072 m for 125 kg. The corresponding X and Y axis response are obtained in Fig. 13. The velocities were illustrated in Figs. 14a, 14b for both of linear and rotary.

4.3 Circle Input

The circular trajectory with radius = *1 m* is a popular test in measuring the performance of wheel chair control System. Fig. 15 shows the circle input response applied to the *PSO-P* controller. The tracking response is closer to the input command. The final obtained errors are increased with increasing the dynamic load from approximately 0 to 0.075 m with 10 kg and 55 kg and finally 0.09 for 125. The results show a better performance compared with Martins et al. [22] with trajectory tracking error exhibits a steady-state value of 0.17 m for payload about 10 kg. Also the results show better circuitry shape than the work of Shojaei et al. [23]. Fig. 16 shows the system response error based on circular trajectory with different payloads. While Figs. 17a, 17b illustrates the system Cartesian response based on circular trajectory. Also by comparing the obtained results with the study of Tiep et al. [24] for 10 kg. payload we found little improvement at x-axis steady state error from 0.01136 to 0.001 and nearly similar value in y-axis (about 0.004). Finally Figs. 18a, 18b represents the system velocities based on circular trajectory
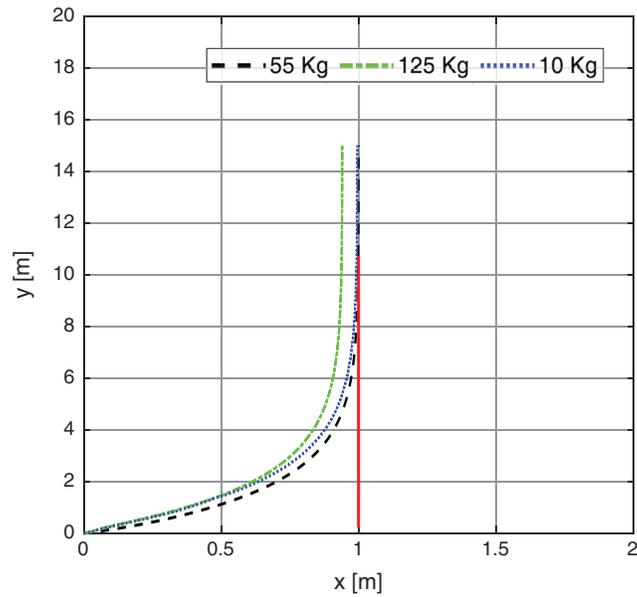
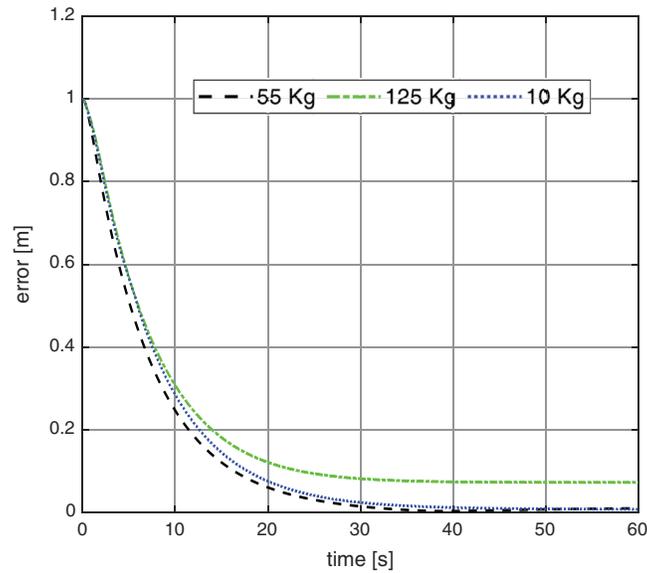**Figure 11:** The system response based on fixed line path with different payloads

Figure 12: The system response error based on fixed line path with different payloads

with different payloads. The previous results of the simulation cleared that PSO strategy can be implemented to adjust control parameters to minimize the system trajectory error successfully. A restriction of the proposed tuning technique is that it depends on the information on the robot dynamic model. In this way, the quality of the tuning results relies upon the nature of the robot model.
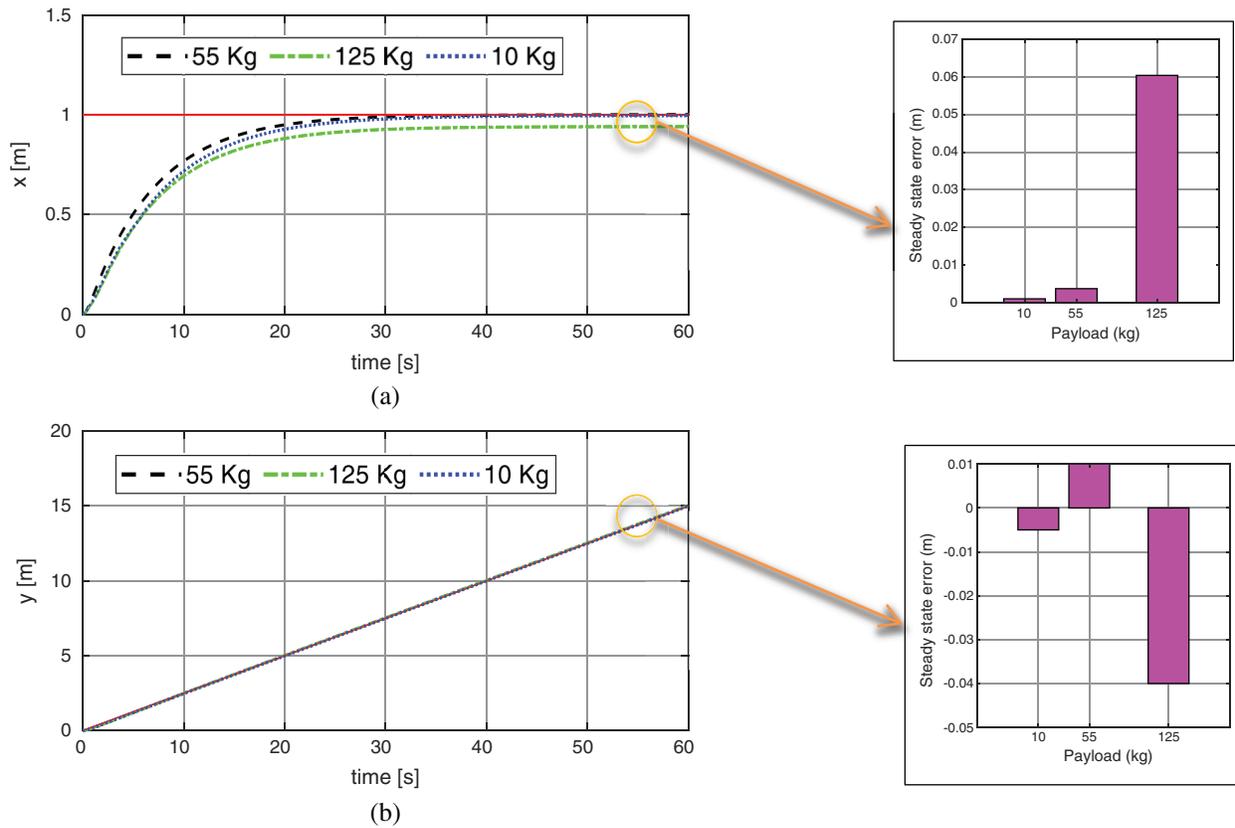
(a)

(b)

Figure 13: The system Cartesian response based on fixed line path with different payloads: (a) X-axis; (b) Y axis
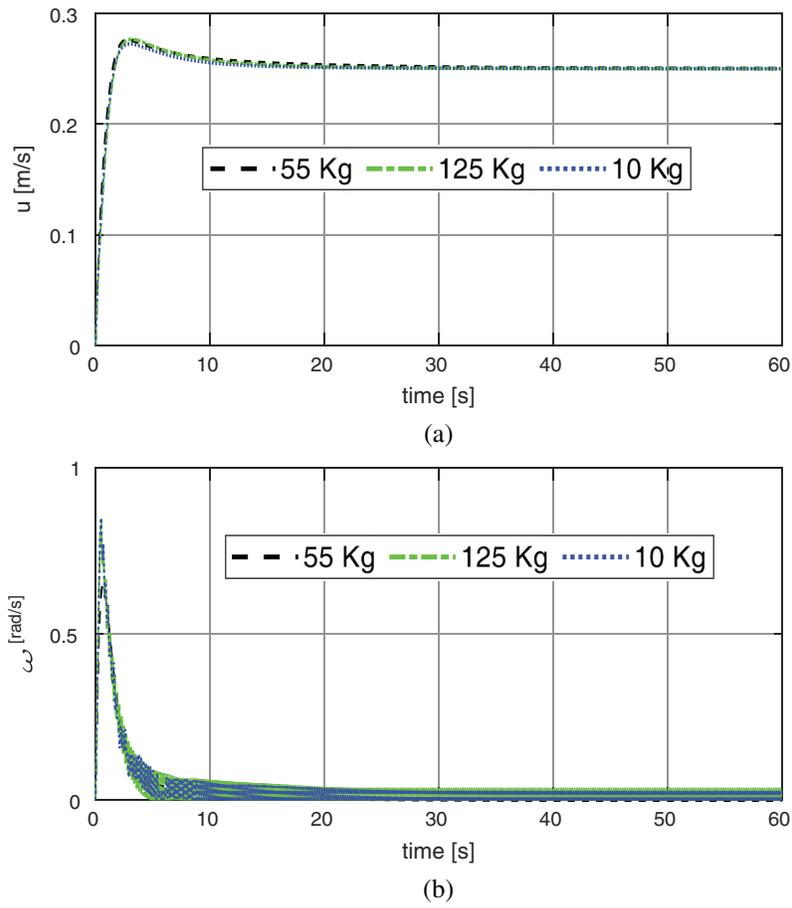
Figure 14: The system velocities based on fixed line reference with different payloads: (a) Linear velocity; (b) Rotary velocity
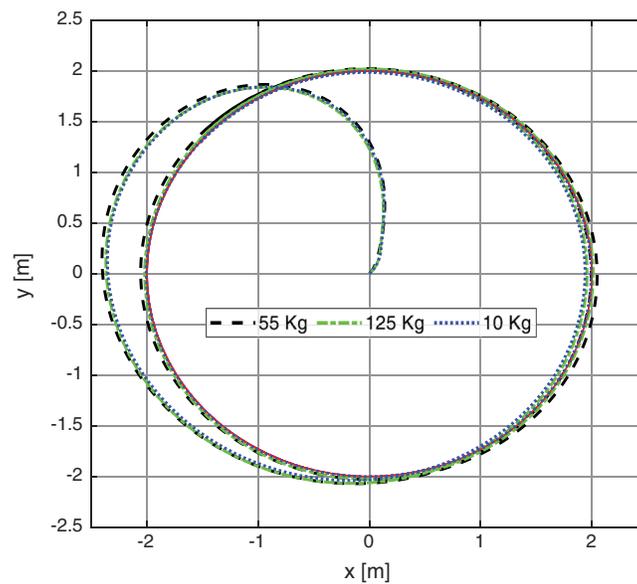

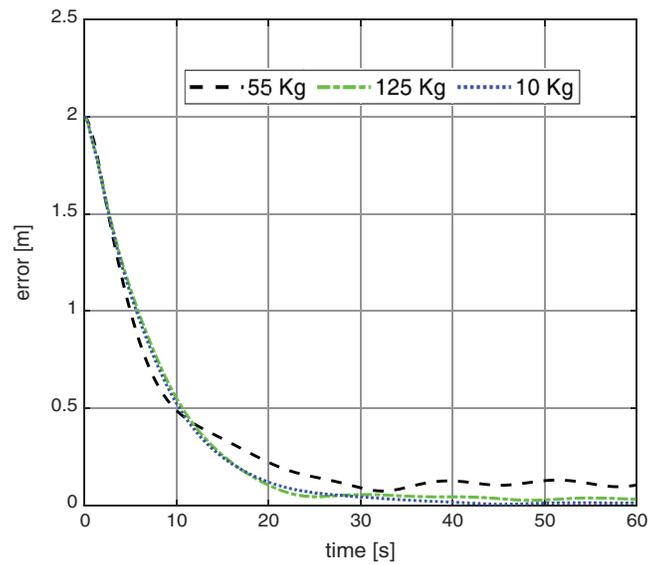**Figure 15:** The system response based on circular trajectory with different payloads

Figure 16: The system response error based on circular trajectory with different payloads
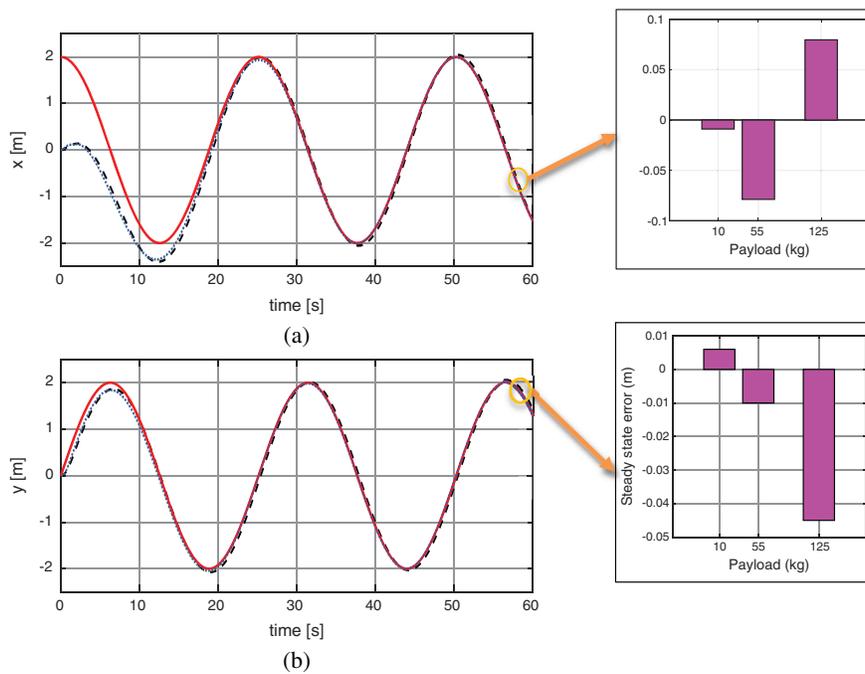

Figure 17: The system Cartesian response based on circular trajectory: (a) X-axis; (b) Y axis
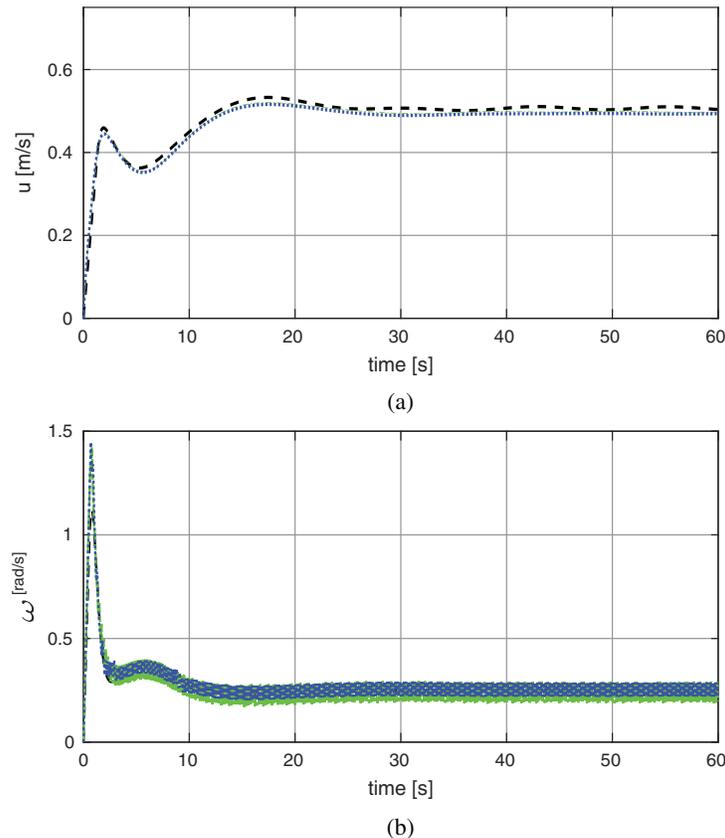
Figure 18: The system velocities based on circular trajectory with different payloads: (a) Linear velocity; (b) Rotary velocity

5 Conclusions

This article presented a tuning method based on the *PSO* algorithm for tune classical proportional control to track the given wheel chair reference motion. The gain concerning the proportional control was adjusted utilizing *PSO* methodology. In order to evaluate effects dynamic load variations, three different payloads were employed with the same *PSO-P* control gain. The presence of steady state error is found with different trajectories references. Therefore, the *PSO-P* controller can accomplish good accuracy with 10 kg and 55 kg loads. It is assured that the *PSO-P* control has effective performance in control of wheel chair system and provides a better performance compared with the previous similar work. Besides, application of the proportional control adjusting with *PSO* is a lot simpler than the customary strategies in light of the fact that there is need neither derivative calculations nor complex mathematical computations.

It has the advantages of rapid respond, tracking accuracy and good anti-interference, so the *PSO-P* controller is the appropriate choice for path tracking control of mobile robots with differential drive

The future work for this study is verifying experimentally the proposed control algorithm to assure its performance with non-predicted dynamic parameters.

Conflicts of Interest: The authors declare that they have no conflicts of interest.

References

[1]   General Authority of Statistics. 2020, Saudi Arabia, https://www.stats.gov.sa/en.

[2]   H. Emam, Y. Hamam, E. Monacelli and I. Mougharbel, "Dynanic model of an electrical wheelchair with slipping detection," in *Proc. of EUROSIM*, Ljubljana, Slovenia, pp. 198–204, 2007.

[3]   M. Gerven, "Modeling and control of an electrically driven wheelchair." M.S. Report, University of Twente, Netherlands, 2006.

[4]   A. Nayyar, V. Puri, N. Nguyen and N. Le, "Smart surveillance robot for real-time monitoring and control system in environment and industrial applications," in *Proc. of Information Systems Design and Intelligent Applications*, Singapore: Springer, pp. 229–243, 2018.

[5]   S. O. Onyango, Y. Hamam, M. Dabo, K. Djouani and G. Qi, "Dynamic control of an electrical wheelchair on an incline," in *Proc. of IEEE AFRICON'09*, Nairobi, Kenya, pp. 1–6, 2009.

[6]   R. Kirby, S. Atkinson and E. MacKay, "Static and dynamic forward stability of occupied wheelchairs: Influence of elevated footrests and forward stabilizers," *Archives of Physical Medicine & Rehabilitation*, vol. 70, no. 9, pp. 681–686, 1989.

[7]   R. Kirby, A. McLean and B. Eastwood, "Influence of caster diameter on the static and dynamic forward stability of occupied wheelchairs," *Archives of Physical Medicine & Rehabilitation*, vol. 73, no. 1, pp. 73–77, 1992.

[8]   K. E. Brown, R. M. Inigo and B. W. Johnson, "Design, implementation, and testing of an adaptable optimal controller for an electric wheelchair," *IEEE Transaction on Industry Applications*, vol. 26, no. 6, pp. 1144–1157, 1990.

[9]   H. Shu and Y. Pi, "Decoupled temperature control system based on PID neural network," in *Proc. of 5th Int. Conf. on ACSE*, Cairo, Egypt, pp. 124–132, 2005.

[10] D. Le, "A new ant algorithm for optimal service selection with end-to-end QoS constraints," *Journal of Internet Technology*, vol. 18, no. 5, pp. 1017–1030, 2017.

[11] J. Kennedy and R. Eberhart, "Particle swarm optimization," in *Proc. of the IEEE Int. Conf. on Neural Networks*, Perth, WA, Australia, vol. 4, pp. 1942–1948, 1995.

[12] R. Eberhart and J. Kennedy, "A new optimizer using particle swarm theory," in *Proc. 6th Int. Sym. on Micro Machine and Human Science*, Nagoya, Japan, pp. 39–43, 1995.

[13] X. D. Cai and Z. Y. Xu, "Weighted next reaction method and parameter selection for efficient simulation of rare events in biochemical reaction systems," *Journal of Chemical Physics*, vol. 124, no. 5, pp. 44–59, 2006.

[14] V. Mukherjee and S. P. Ghoshal, "Comparison of intelligent fuzzy based AGC coordinated PID controlled and PSS controlled AVR system," *International Journal of Electrical, Power & Energy Systems*, vol. 29, no. 9, pp. 679–689, 2007.

[15] A. A. Aly, "PID parameters optimization using genetic algorithm technique for electrohydraulic servo control system," *Intelligent Control and Automation*, vol. 2, no. 2, pp. 69–76, 2011.

[16] O. Hassanein and A. Aly, "Genetic-PID control for a fire tube boiler," in *Proc. of the 2nd IEEE Int. Conf. on Computational Cybernetics ICCC*, Vienna, pp. 19–24, 2004.

[17] A. Aly and S. Elnaggar, "Genetic PD control of a three-link rigid spatial manipulator," *International Journal on Automatic Control System Engineering*, vol. 11, no. 1, pp. 15–22, 2011.

[18] F. Martins, C. Celeste, R. Carelli, M. Sarcinelli and F. Bastos, "Kinematic and adaptive dynamic trajectory tracking controller for mobile robots," in *Proc. 3rd Int. Conf. on Advances in Vehicle Control and Safety AVCS'07*, Buenos Aires, Argentina, pp. 1354–1363, 2007.

[19] Eberhart and Y. Shi, "Particle swarm optimization: Developments, applications and resources," in *Proc. Congress on Evolutionary Computation*, Seoul, South Korea, pp. 81–86, 2001.

[20] R. C. Simpson, "Smart wheelchairs: A literature review," *Rehabilitation Research & Development*, vol. 42, no. 4, pp. 423–438, 2005.

[21] K. Pathak, J. Franch and K. Agrawal, "Velocity and position control of a wheeled inverted pendulum by partial feedback linearization," *IEEE Transactions on Robotics*, vol. 21, no. 3, pp. 505–513, 2005.

[22] F. N. Martins, W. C. Celeste, R. Carelli, M. Sarcinelli-Filho and T. F. Bastos-Filho, "An adaptive dynamic controller for autonomous mobile robot trajectory tracking," *Control Engineering Practice*, vol. 16, no. 1, pp. 1354–1363, 2008.

[23] K. Shojaei, A. M. Shahri, A. Tarakameh and B. Tabibian, "Adaptive trajectory tracking control of a differential drive wheeled mobile robot," *Robotica*, vol. 29, no. 1, pp. 391–402, 2011.

[24] D. K. Tiep, K. Lee, D. Y. Im, B. Kwak and Y. J. Ryoo, "Design of fuzzy-PID controller for path tracking of mobile robot with differential drive," *International Journal of FUZZY LOGIC and Intelligent Systems*, vol. 18, no. 3, pp. 220–228, 2018.